Ultrastructural Localization of the Herpes Simplex Virus Type 1 U_L31, U_L34, and U_S3 Proteins Suggests Specific Roles in Primary Envelopment and Egress of Nucleocapsids

Ashley E. Reynolds,[1] Elizabeth G. Wills,[1] Richard J. Roller,[2]
Brent J. Ryckman,[2] and Joel D. Baines[1]*

*Department of Microbiology and Immunology, Cornell University, Ithaca, New York 14853,[1] and
Department of Microbiology, University of Iowa, Iowa City, Iowa 52242[2]*

The wild-type U_L31, U_L34, and U_S3 proteins localized on nuclear membranes and perinuclear virions; the U_S3 protein was also on cytoplasmic membranes and extranuclear virions. The U_L31 and U_L34 proteins were not detected in extracellular virions. U_S3 deletion caused (i) virion accumulation in nuclear membrane invaginations, (ii) delayed virus production onset, and (iii) reduced peak virus titers. These data support the herpes simplex virus type 1 deenvelopment-reenvelopment model of virion egress and suggest that the U_S3 protein plays an important, but nonessential, role in the egress pathway.

Herpes simplex virus type 1 (HSV-1) virions contain a linear double-stranded DNA genome of approximately 152 kb that is packaged into an icosahedral capsid shell. An amorphous tegument layer surrounds the capsid and is, in turn, surrounded by an envelope composed of a host-derived lipid bilayer studded with viral integral membrane proteins. After the viral genome is replicated and packaged into capsids within the nucleus, assembled nucleocapsids acquire a primary lipid envelope by budding through the inner nuclear membrane (INM) into the space located between the inner and outer leaflets of the nuclear envelope (25, 33). Whereas the derivation of the primary envelope from the INM is widely accepted, the route of transit of the nascent virions from the perinuclear space to the extracellular space is more controversial. An overview of the key players in herpesvirus egress and a comparison of the salient features of the two proposed envelopment models have been recently published (8, 25).

A single-step model of herpesvirus envelopment was proposed for the prototypical alphaherpesvirus HSV-1 (6, 18, 35, 44). This model proposes that enveloped virions move through the endoplasmic reticulum (ER) and the Golgi apparatus in transport vesicles with concomitant modification of primary virion glycoproteins. The single-step envelopment model is supported by the observations that (i) enveloped particles within vesicles can be readily detected by electron microscopy and in fracture label studies (35, 44) and (ii) virion egress and virion-associated glycoprotein processing are both inhibited in cells treated with the ionophore monensin (18). On the other hand, neither of these observations can exclude the alternative deenvelopment-reenvelopment model. Such a model is supported by mounting ultrastructural and biochemical evidence (3, 10, 13, 14, 30, 37, 41, 46, 50) and has been proposed for HSV-1, other alphaherpesviruses such as varicella-zoster virus

(VZV) and pseudorabies virus (PrV), and betaherpesviruses such as human cytomegalovirus. In this model, primary envelopment occurs by budding through the INM but the primary envelope surrounding the perinuclear virion is lost, presumably by fusion with the outer lamellae of the nuclear envelope. In a second step, reenvelopment occurs by wrapping of the nucleocapsid and its associated tegument with a lipid bilayer originating from a membranous cytoplasmic organelle bearing viral glycoproteins previously modified by transit through the normal secretory pathway. It has been proposed that the second envelope is derived from membranes that normally reside within the trans-Golgi network or other Golgi membranes (3, 11, 24, 47, 50).

Several proteins have been implicated in the initial budding of herpesvirus nucleocapsids at the INM, including the HSV U_L11, U_L31, and U_L34 proteins, along with glycoprotein K, a protein necessary for envelopment in nondividing cells (1, 15, 16). Studies done in our laboratories previously demonstrated that the U_L31 and U_L34 gene products of HSV-1 form a complex that is targeted to the nuclear rim and is essential for optimal primary envelopment of nucleocapsids (32, 34). Similar results have been obtained upon analysis of the U_L31 and U_L34 homologues of PrV (10, 21).

The U_L31 gene product is a nuclear matrix-associated, nucleotidylylated phosphoprotein that, in association with the U_L34 gene product, localizes to the nuclear rim of HSV-1-infected cells (2, 4, 32, 48). The U_L34 gene product is a nuclear membrane-associated phosphoprotein with a predicted type II integral membrane topology. Also, U_L34 protein is a substrate for the HSV-1 U_S3-encoded kinase (9, 28, 29, 34, 36, 49). As demonstrated by Reynolds et al. (32), U_S3 kinase is required for even distribution of the U_L31 and U_L34 proteins around the nuclear rim of wild-type-infected cells. In addition, the U_S3-encoded kinase has been proposed to play a role in protecting HSV-1-infected cells from virus-induced apoptosis (17, 23). In the absence of the PrV U_S3 protein homologue, large numbers of enveloped virions appear to accumulate within invaginations of the nuclear membrane (22, 45). These data led

* Corresponding author. Mailing address: Department of Microbiology and Immunology, Cornell University, Veterinary Medical Center (VMC) C5 131, Ithaca, NY 14853. Phone: (607) 253-3385. Fax: (607) 253-3384. E-mail: jdb11@cornell.edu.

TABLE 1. Summary of the distribution of U_L31 protein determined by immunogold analysis of thin sections[a]

Virus[b]	Total no. of gold beads counted in 10 whole-cell sections	No. (%) of gold beads in:		
		Nuclear membrane	Nucleoplasm	Cytoplasm
Wild type	312	21.6 ± 3.0 (69.2)	5.4 ± 0.7 (17.3)	4.2 ± 1.0 (13.5)
U_L34 null	1,104	38.1 ± 4.5 (34.5)	37.0 ± 5.2 (33.5)	35.3 ± 6.7 (32.0)
U_S3 null	2,295	127.7 ± 29.6 (55.6)	52.7 ± 10.0 (23.0)	49.1 ± 14.8 (21.4)
U_L31 null	39	0.6 ± 0.2 (15.4)	2.4 ± 0.7 (61.5)	0.9 ± 0.3 (23.1)

[a] The total numbers of gold beads in 10 randomly selected whole-cell sections of wild-type virus [HSV-1(F)], U_L31-null virus-, U_L34-null virus-, and U_S3-null virus-infected cells were quantified. The mean number of U_L31 protein-specific gold beads and the standard error of each mean are indicated for three regions of the cells. The following formula was used to calculate the percentage of gold beads in a given region of the cell infected with the indicated virus: (number of gold bead particles per region of 10 whole-cell sections/total number of gold bead particles in 10 whole-cell sections) × 100 = % of gold beads per region.

[b] Ten samples of each virus were tested

to the deduction that the U_S3-encoded kinase is also important for the efficient deenvelopment of nascent virions that occurs upon fusion of the virion envelope with the outer nuclear membrane (ONM).

The goal of this study was to determine the localization of the HSV-1 U_S3, U_L31, and U_L34 proteins in infected cells at the ultrastructural level. Consistent with the deenvelopment-reenvelopment model of virion egress, U_L31 and U_L34 proteins were observed to associate with perinuclear virions but not with extracellular virions. The localization of the HSV-1 U_S3-encoded kinase in infected cells and the phenotype of cells infected with the U_S3-null mutant virus provide support for the hypothesis that one of several potential roles of U_S3 kinase is to promote efficient egress of virions from the nucleus into the cytoplasm.

The cell lines used for this study were previously described (31, 43). The wild-type HSV-1(F) virus and U_S3 mutants R7037 and R7039 (provided by Bernard Roizman, University of Chicago) have been previously characterized (7, 29). R7037 contains a deletion of portions of the U_S3 and U_S4 open reading frames (ORFs), and R7039 contains a deletion of portions of the U_S2 and U_S3 ORFs. The construction and growth properties of HSV-1(F) U_L34-null mutant vRR1072 (tk⁺) have been described previously (34). U_L31-null mutant virus R5132, also provided by Bernard Roizman, has been described previously (5). Both vRR1072 (tk⁺) (U_L34-null mutant virus) and R5132 (U_L31-null mutant virus) were propagated on stably transfected, complementing cell lines as detailed previously (32).

The following protocol was utilized for all immunogold electron microscopy. Vero cells were infected at a multiplicity of infection (MOI) of 5 and maintained at 37°C until harvesting at 14 to 18 h postinfection (hpi). The viral inoculum used for each preparation was diluted in 199V medium (199 medium supplemented with 1% newborn calf serum, penicillin, and streptomycin [43]). Harvested cells were pelleted by centrifugation and fixed with 4% formaldehyde and 0.25% glutaraldehyde in 0.1 M sodium phosphate buffer (pH 7.4) for 30 min at 25°C and then for 90 min at 4°C. Fixed cells were washed three times for 10 min per wash in phosphate-buffered saline (PBS) at 4°C, dehydrated with increasing ethanol concentrations at 4 and −20°C, and embedded stepwise at −20°C with increasing concentrations of LRWhite (Electron Microscopy Sciences, Fort Washington, Pa.). The samples were then polymerized under UV light at −35°C overnight.

U_L31 protein is predominantly localized to the nuclear membrane of HSV-1(F)-infected cells. Thin sections were prepared for immunogold electron microscopy as described above and probed with U_L31 protein-specific rabbit polyclonal antiserum that was prepared as described previously and diluted 1:2 (31, 32). Donkey anti-rabbit immunoglobulins conjugated with 12-nm-diameter colloidal gold particles were incubated with the thin sections for 1 h (electron microscopy grade 12-nm colloidal gold AffiniPure donkey anti-rabbit immunoglobulin G [IgG]; catalog no. 711-205-152; Jackson ImmunoResearch Laboratories, Inc., West Grove, Pa.). Excess antibodies were removed by washing with PBS-Tween 80–1% fish gelatin. Postlabeling fixation was performed with 2.5% glutaraldehyde in 0.1 M phosphate buffer for 10 min and followed by rinsing with distilled water. Sections were counterstained with 2% uranyl acetate and lead citrate, coated with Formvar (0.5% Formvar in ethylene dichloride; Ladd Research Industries, Williston, Vt.), and examined with a Philips 201 transmission electron microscope. Conventionally rendered negatives of electron microscopic images were scanned with ScanWizard Pro PPC 1.02 software (Microtek, Redondo Beach, Calif.), and digital images were generated with Adobe Photoshop 5.0 software.

The distribution of U_L31 protein in cells infected with various viral strains analyzed by transmission electron microscopy (TEM) is summarized in Table 1. Statistical analysis of the means and standard errors of the means presented in Table 1 was done by PROC UNIVARIAT utilizing SAS (Statistical Analysis Systems).

Colloidal gold beads representing the localization of U_L31 protein were detected lining the INM and, to a lesser extent, the ONM of cells infected with HSV-1(F), as seen in Fig. 1A and B. The U_L31 gene product was also associated with enveloped viral particles located between the lamellae of the nuclear envelope. Ten randomly selected whole-cell sample sections were counted, and approximately two-thirds of the gold beads were associated with parts of the nuclear rim (in the INM, in the ONM, between leaflets in the perinuclear space, and within cytoplasmic and nuclear sites directly adjacent to the nuclear membrane leaflets) or with viral particles that associated with these sites. Approximately 1/5 of the gold particles were associated with the central nucleoplasm, and approximately 1/10 of the particles were localized free in the cytosol, on cytoplasmic structures, or in association with cytoplasmic or extracellular virions (Fig. 1C).

In cells infected with the U_L31 deletion virus and harvested at time points comparable to those of experiments with wild-type virus-infected cells (Fig. 2A), very few viral particles were
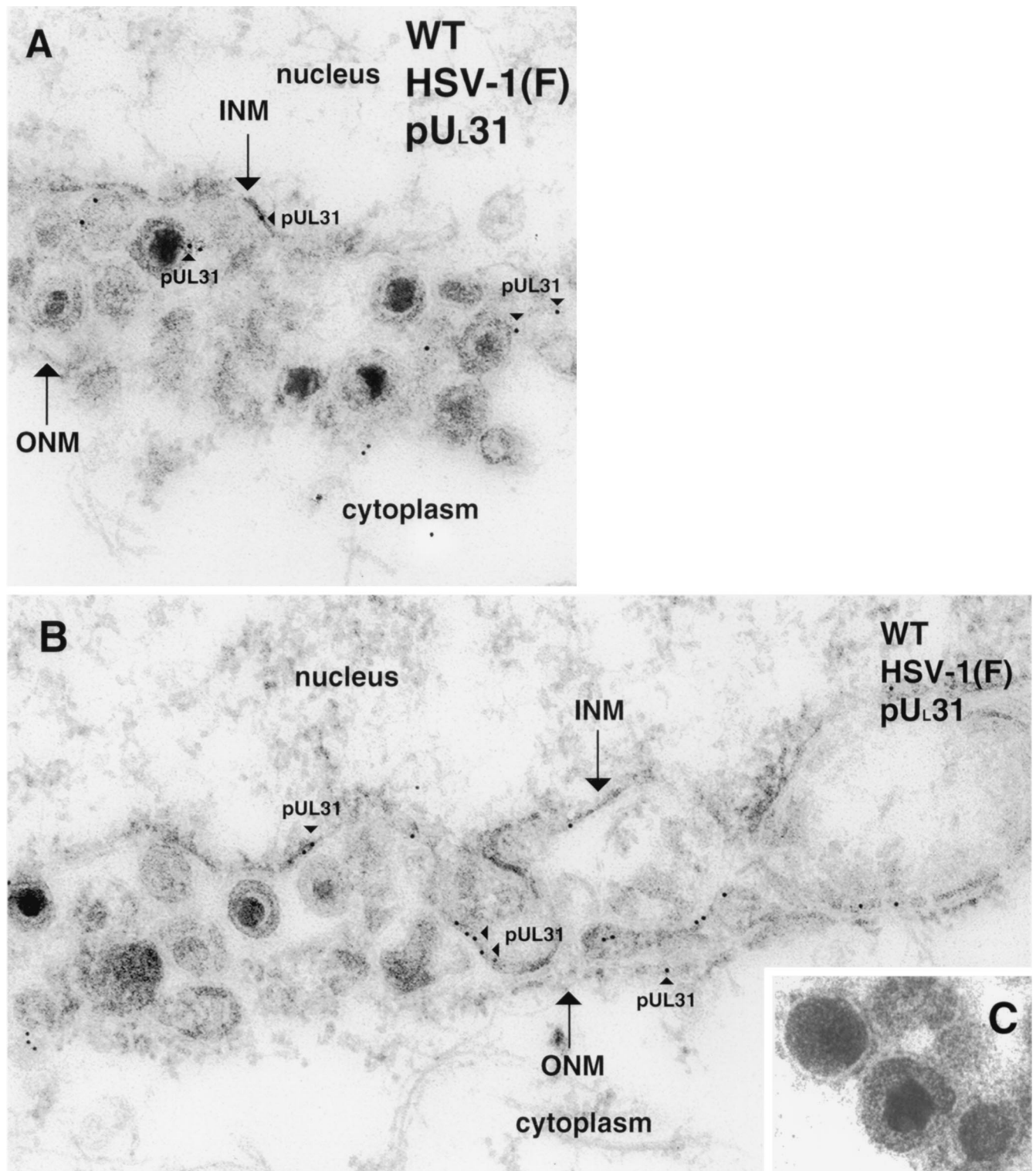
FIG. 1. Digitally scanned electron micrograph of thin sections of wild-type (WT) HSV-1(F)-infected Vero cells harvested and fixed 14 to 18 hpi. The nucleus, INM, ONM, and cytoplasm are labeled in panels A and B. Gold beads associated with the U_L31 protein (pU_L31) are demarcated with arrowheads. Panel C demonstrates extracellular virions devoid of pU_L31-specific immunogold label. For reference, in the electron micrographs presented here, HSV-1 nucleocapsids are approximately 120 nm in diameter and gold beads are 12 nm in diameter. Original magnification of panels A to C, ×45,000.
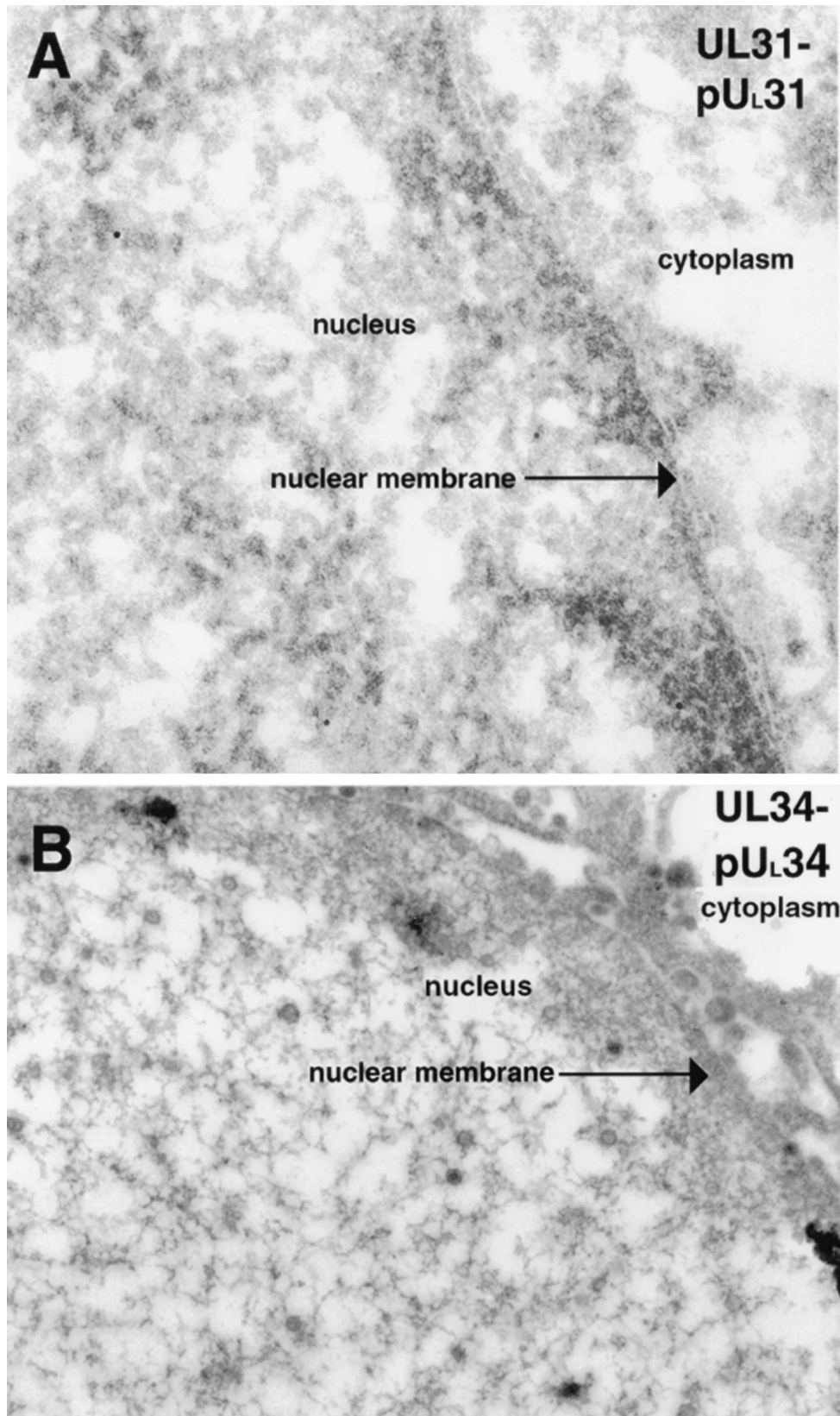
FIG. 2. Scanned digital electron micrograph of U_L31-null mutant virus-infected thin sections of Vero cells (A) or U_L34-null mutant virus-infected thin sections of Vero cells (B) harvested and fixed late in infection (14 to 18 hpi). In panel A, thin sections were probed with U_L31-specific rabbit antisera. The cytoplasm, nuclear membrane, and nucleus are all labeled. Original magnification of panel A, ×45,000. In panel B, thin sections were probed with U_L34 protein-specific IgY antibodies. Original magnification of panel B, ×45,000.

located outside of the nucleus, in contrast to the appearance of cells infected with HSV-1(F). This indicated that the U_L31 protein, while not absolutely essential for egress of nascent virions from the nucleus, greatly facilitated the process. Upon staining of sections of cells infected with the U_L31 deletion virus with the U_L31 protein-specific rabbit polyclonal antiserum, it was apparent that nonspecific staining with the U_L31 polyclonal antisera was minimal, yielding a mean value of approximately four gold beads per cross section of an entire cell (averaged from 10 randomly selected sections counted). Wild-type virus-infected cells had, on average, a mean of approximately 31 gold beads per whole-cell cross section (averaged from 10 random whole-cell sections counted).

The difference in the quantity of gold beads detected at the nuclear membranes between cells infected with the wild-type virus and the U_L31-null mutant was particularly striking. Whereas the mean number of gold particles at the nuclear membranes of wild-type virus-infected cells was approximately 22, in a sample size of 10 whole-cell sections selected at random, the nuclear membrane of U_L31-null virus-infected cells had a mean of only 0.6 gold bead per section (averaged from the 10 random cell sections counted). Thus, we deduced that the immunoreactivity detected in HSV-1(F)-infected cells at the nuclear membrane was specifically attributable to the presence of the U_L31 gene product.

The U_L34 gene product is detectable on the INM and ONM of cells infected with HSV-1(F). Thin sections of cells infected with HSV-1(F) were prepared as described above and reacted with an affinity-purified chicken IgY antibody directed against the U_L34 protein diluted 1:50 in 1% cold bovine serum albumin-PBS (32). Donkey anti-chicken IgY antibodies conjugated with 12-nm-diameter colloidal gold particles were incubated with the sections probed with the U_L34 protein-specific chicken IgY antibody for 1 h (electron microscopy grade 12-nm colloidal gold AffiniPure donkey anti-chicken IgY; catalog no. 703-205-155; Jackson ImmunoResearch). Stained sections were prepared as described above and subsequently examined by TEM. Representative results are shown in Fig. 3. Immunostaining with the U_L34 antibody was considerably more intense than was U_L31 protein-specific immunostaining, and hundreds of beads were visible in a given section of a whole cell (Fig. 3A). Unlike the U_L31 protein, where the majority of the gold beads were localized on the INM, colloidal gold particles representing the localization of the U_L34 protein were detected in approximately equal amounts on the INM and ONM, as shown in Fig. 3C. Additional immunoreactivity specific for the U_L34 protein was detectable on perinuclear viral particles (Fig. 3B). As was the case with the U_L31 protein, U_L34 protein-specific immunoreactivity was not observed in association with structures in the cytoplasmic compartment, cytoplasmic viral particles, or virions in the extracellular space (Fig. 3D). As a negative control, U_L34-null mutant virus-infected cells were harvested at time points comparable to those of the wild-type virus-infected cells and incubated with the U_L34 antibodies (Fig. 2B). Minimal background staining was detected by immunogold analysis, and we therefore concluded that the staining seen in wild-type HSV-1(F)-infected cells incubated with anti-U_L34 IgY antibodies was specific for U_L34 protein epitopes. It is noteworthy that by immunogold analysis, neither the U_L31 nor the U_L34 protein was detectable in as-

sociation with cytoplasmic or extracellular viral particles. Similarly, the PrV-encoded homologues of these proteins are not present at detectable levels on intracytoplasmic or extracellular particles but are readily detectable on perinuclear particles (10, 21). Previous studies demonstrated that low levels of the HSV-1 U_L34 protein are detectable in virions purified from cytoplasmic extracts (29). This observation is consistent with our immunogold analyses inasmuch as cytoplasmic virion preparations would be expected to contain some virions purified from the perinuclear space that contain the U_L34 protein. Although our studies do not necessarily rule out the possibility that the U_L31 and U_L34 proteins are present in extracellular virions, the very strong immunoreactivity associated with nascent viral particles, compared with the virtual absence of immunoreactivity in extracellular particles, indicates that the two particle types, perinuclear and extracellular, differ significantly in U_L31 and U_L34 protein content. Such observations provide strong evidence that during egress of viral particles, the initial, INM-derived envelope containing the integrated U_L34 protein is removed and reenvelopment provides a novel envelope lacking (or containing drastically decreased levels of) the U_L34 protein. These data are most consistent with a model in which the membrane acquired during primary envelopment is lost by fusion with the ONM and deenveloped viral particles are released into the cytoplasm, where the particles are wrapped in a new envelope derived from the Golgi apparatus or another membranous organelle.

The presence of both the U_L31 and U_L34 proteins on virus particles located between the lamellae of the nuclear membrane is the first evidence supporting our previous hypothesis that the U_L31/U_L34 protein complex becomes incorporated into virions upon budding at the INM (32). We hypothesize that the U_L31/U_L34 complex at the INM engages nucleocapsids, causing them to accumulate at the nuclear envelope and subsequently undergo primary envelopment. When budding of nucleocapsids through the INM occurs, nascent virions labeled with the U_L31 and U_L34 proteins accumulate in the perinuclear space, as shown in Fig. 1 and 3. We predict that, in the absence of either protein, nucleocapsids will not be effectively retained at the nuclear rim and, consequently, envelopment of nucleocapsids will not occur efficiently.

U_L31 protein localization in cells infected with the U_L34 deletion virus. As described previously (32), the U_L34 protein plays a crucial role in maintenance of the U_L31 protein at the nuclear rim of wild-type virus-infected cells. This was confirmed by immunogold analyses. In cells infected with the U_L34 deletion virus, the level of U_L31 protein-specific immunoreactivity was approximately evenly distributed among the nuclear membrane, the nucleoplasm, and the cytoplasm. The results are summarized in Table 1.

The U_L34 protein is not strictly associated with the nuclear rim in U_L31-null mutant virus-infected cells. Thin sections of cells infected with the U_L31-null mutant were also reacted with the U_L34 protein-specific antisera, and bound antibody was detected by reaction with gold bead-conjugated anti-chicken antisera. Examination of the samples by TEM revealed that U_L34 protein-specific immunoreactivity localized primarily at the INM and ONM. Unlike the appearance of cells infected with the wild-type virus, U_L34 protein-specific immunoreactivity was also associated with regions of the cytoplasm in a
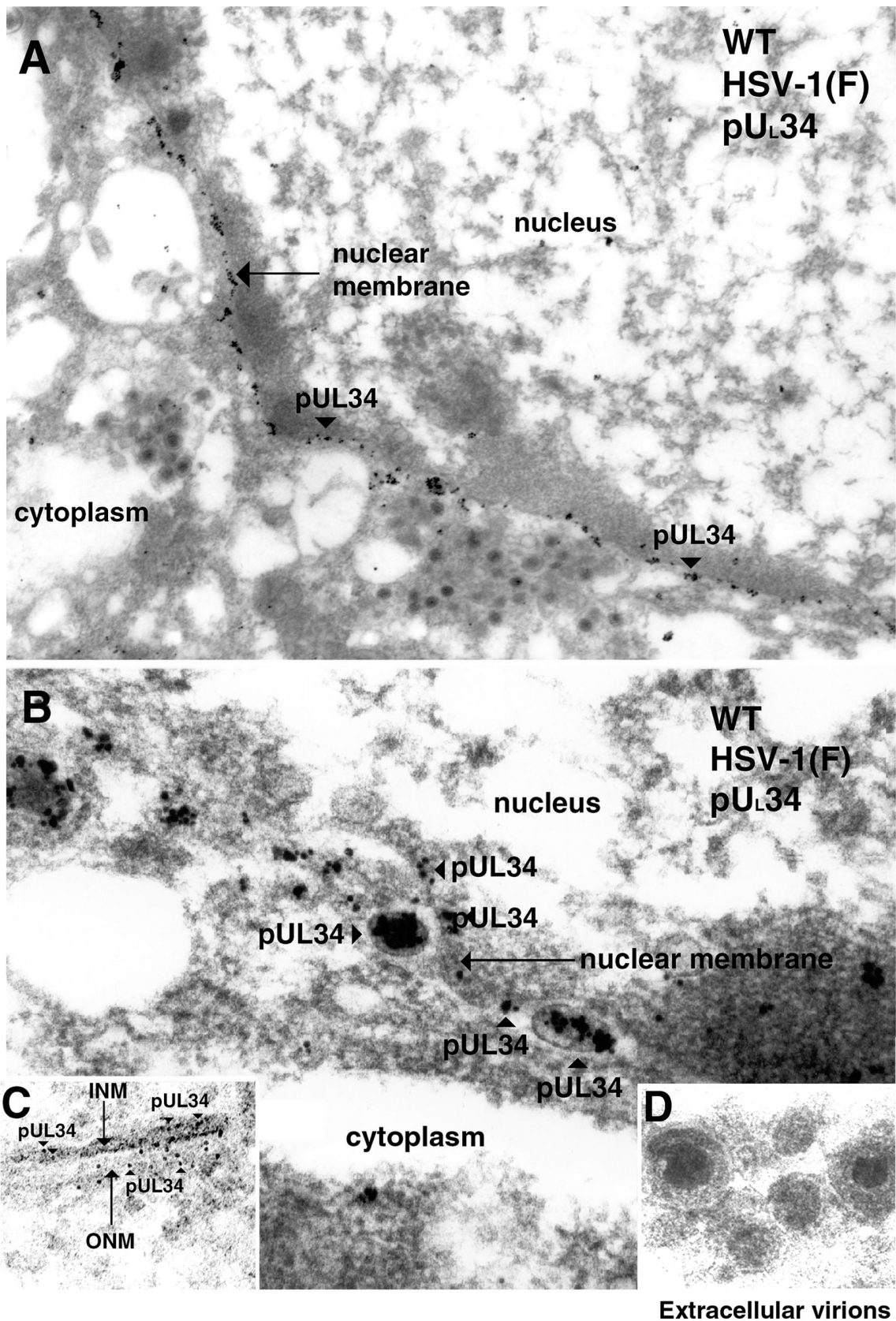
FIG. 3. Scanned digital electron micrograph of thin sections of wild-type(WT) virus-infected Vero cells harvested and fixed late in infection. Thin sections were incubated with U_L34 protein-specific chicken IgY antibody. The nucleus, nuclear membrane, and cytoplasm are labeled in panel A and, in panels B and C, the INM and ONM are indicated with arrows, as are the cytoplasm and nucleus. Panel D shows extracellular virions probed with U_L34 antisera devoid of gold label. Regions labeled with U_L34 protein-specific antisera are demarcated with arrowheads labeled pU_L34. Original magnification of panels A to D, ×45,000.

largely perinuclear distribution (data not shown). A minor portion of the total detectable U_L34 protein immunoreactivity was observed within the nucleoplasm (data not shown).

Previous studies by Reynolds et al. (32) characterizing the distribution of the U_L31 protein in U_L34-null mutant virus-infected cells by indirect immunofluorescence assay (IFA) also demonstrated that the U_L31 protein is mislocalized from the nuclear rim and is localized primarily in the central nucleus and, to a lesser extent, in the cytoplasm.

The model of U_L31 and U_L34 localization and function previously proposed by Reynolds et al. (32) was largely based on IFA data. The ultrastructural information gained from the present study demonstrates, for the first time, that both of these HSV-1 proteins associate with the INM, among other structures at the nuclear membrane. Analyses of the cells infected with the U_L31- and U_L34-null mutants indicate that whereas each protein has the capacity to target the nuclear rim region in the absence of the reciprocal protein, association in the INM is optimized in the presence of both proteins in infected cells. Given the previous observation that U_L31 and U_L34 are sufficient to target one another to the nuclear rim in the absence of other HSV-1 proteins (32), it is likely that cellular proteins also contribute to the localization of the U_L31/U_L34 protein complex at the INM. Given the nuclear matrix association of the U_L31 protein (4), it is reasonable to hypothesize that such proteins might include lamins or lamin receptors that normally localize on the nucleoplasmic face of the INM.

The data are consistent with our previously proposed model (32), which was based on the lamin B receptor localization paradigm (38, 39, 40). Briefly, the U_L34 protein integrates itself into the ER membrane in a type II orientation, diffuses laterally along the lipid bilayer into the ONM, which is continuous with the ER, diffuses past the nuclear pore complex (NPC) with its N-terminal domain in the lateral channel of the NPC, and moves to the INM, where the bulk of the protein resides in the nucleoplasm. In HSV-1(F)-infected cells, the INM-bound U_L34 protein encounters the U_L31 gene product, which is targeted to the nucleus by virtue of an N-terminal nuclear localization signal (51). When the U_L34 protein interacts with the U_L31 protein, a complex of the proteins is formed that is predicted to be stably anchored to the nuclear membrane through the transmembrane domain of the U_L34 gene product and the nuclear matrix association of the U_L31 protein.

Subcellular localization of the U_S3-encoded kinase. We have previously reported that the U_S3-encoded kinase and its substrate, the U_L34 protein, colocalize extensively in the absence of other viral factors (32). The subcellular localization of the U_S3-encoded kinase in HSV-1-infected cells has not been reported. Inasmuch as the U_S3 and U_L34 proteins colocalize in transiently transfected cells (32), it was hypothesized that the U_S3 and U_L34 proteins would also colocalize in wild-type-infected cells.

To test this hypothesis, HEp-2 cells were grown to approximately 70% confluence on sterile glass coverslips and infected at an MOI of 10 for 12 h at 37°C with HSV-1(F) or R7039. Infected cells were fixed for 15 min in 2% formaldehyde–PBS, washed three times in PBS, and permeabilized for 15 min in immunofluorescence (IF) buffer as previously described (32).

Cells were blocked for 1 h in IF buffer supplemented with 0.01% pooled human immunoglobulins, washed three times in PBS, reacted for 1 h with primary antibodies diluted in IF buffer, washed three times in PBS, and then reacted for 1 h with secondary antibodies diluted in IF buffer. Chicken anti-U_L34 antibody was diluted 1:4,000, rabbit anti-U_S3 antibody (26) was diluted 1:1,000, and donkey anti-chicken immunoglobulin-Texas Red conjugate and goat anti-rabbit immunoglobulin-fluorescein isothiocyanate conjugate were both diluted 1:200. Immunostained cells were analyzed by confocal microscopy as previously described (32). The results are shown in Fig. 4.

As previously demonstrated by Reynolds et al. (32), in cells infected with a U_S3-null virus, the U_L34 protein was detected in a punctate distribution at the nuclear envelope (Fig. 4A). This is in stark contrast to cells infected with HSV-1(F), where the U_L34 protein adopted a more uniformly even distribution at the nuclear envelope (Fig. 4D). In HSV-1(F)-infected cells, the U_S3-encoded kinase was detected at the plasma membrane, in cytoplasmic structures, and at the nuclear envelope, where it colocalized with the U_L34 protein (Fig. 4E and F). Areas of colocalization of the two proteins appear yellow in these merged images. The localization of the U_S3 protein at the nuclear rim (marked with a white arrowhead in Fig. 4E) and the plasma membrane (marked with a long white arrow in Fig. 4E) was never seen in cells infected with the U_S3-null virus and is distinct from the largely cytoplasmic background fluorescence detected in cells infected with that virus, demonstrating that these are sites of specific anti-U_S3 reactivity (Fig. 4B). Some of the background fluorescence detected in Fig. 4B may be attributable to incomplete blocking of the virus-encoded Fc receptor (a complex of glycoproteins E and I [19]) despite the use of pooled human immunoglobulins as a blocking agent. The presence of the background fluorescence does not permit any conclusion to be drawn about U_S3 protein localization in the cytosol or on cytoplasmic membranes as determined by IFA. These IFA data indicate that the U_S3 protein localizes to the plasma membrane and the nuclear envelope, where it colocalizes with the U_L34 protein (Fig. 4E and F). In view of the previous report that the U_S3 and U_L34 proteins colocalize in transiently transfected cells (32), we therefore hypothesize that the U_S3-encoded kinase and its substrate, the U_L34 protein, may physically and stably interact.

While the relationship between the localization of the U_L34 protein and that of the U_S3 protein in other alphaherpesviruses has not been addressed, studies of the localization of PrV and HSV-2 U_S3 homologues have detected them diffusely distributed throughout infected cells (12, 22).

The HSV-1 U_S3-encoded kinase localization in infected cells and association with extracellular particles are markedly different from the distribution of the U_L31 and U_L34 proteins. To characterize the localization of the U_S3-encoded kinase at the ultrastructural level, thin sections of cells infected with HSV-1(F) or the U_S3-null mutant R7037 were reacted with a U_S3-specific rabbit polyclonal antiserum (supplied by Bernard Roizman) (26) diluted 1:10 in cold bovine serum albumin-PBS and bound IgG was detected as described for the U_L31 protein. Representative results are shown in Fig. 5.

Like the distribution of the U_L34 protein in HSV-1(F)-infected cells, the U_S3 protein was associated with both lamel-
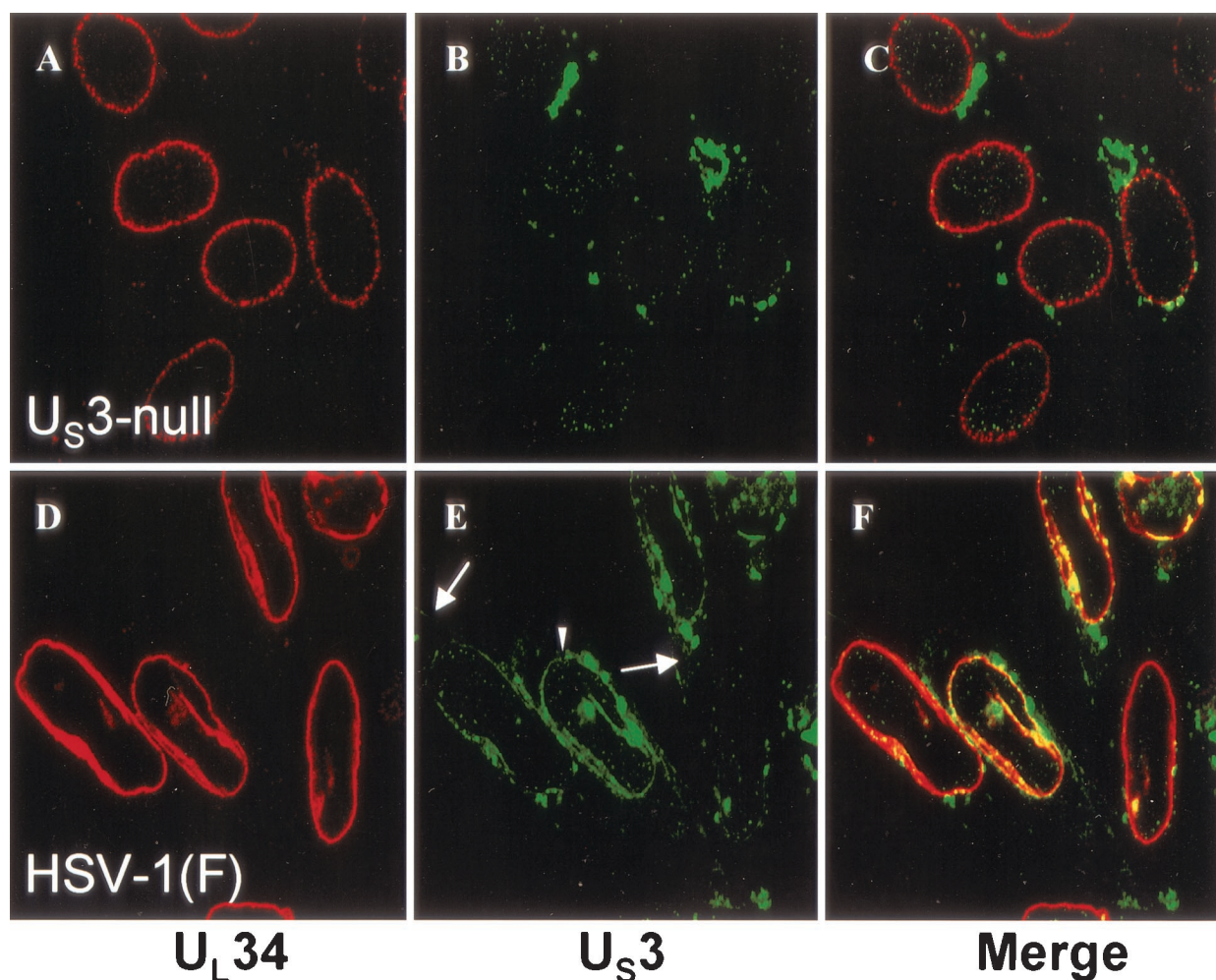
FIG. 4. Digital confocal images showing localization of the U$_L$34 and U$_S$3 proteins in HEp-2 cells infected with HSV-1(F) or U$_S$3-null HSV-1. Subconfluent monolayers of HEp-2 cells were infected for 12 h with either U$_S$3-null mutant virus R7039 (A to C) or HSV-1(F) (D to F). Formaldehyde-fixed cells were immunostained with chicken anti-U$_L$34 antibody that was detected with donkey anti-chicken IgG-Texas Red conjugate (red), and rabbit anti-U$_S$3 antibody was detected with goat anti-rabbit IgG-fluorescein isothiocyanate conjugate (green). The long white arrow indicates U$_S$3 protein detected at the plasma membrane, and the white arrowhead indicates U$_S$3 protein detected at the nuclear membrane. Areas of colocalization of the two proteins appear yellow in the merged images (C and F). Original magnification, ×1,000.

lae of the nuclear envelope and with perinuclear viral particles as well. No obvious staining specific for the U$_S$3 protein was detectable in the nucleoplasm of infected cells. Several key differences between the distribution of the U$_S$3 protein and that of the U$_L$31 or U$_L$34 protein were noted. Unlike the appearance of the U$_L$31 or U$_L$34 protein, gold beads demarcating the location of the Us3 protein were detected extensively within the cytoplasm. Cytoplasmic U$_S$3 protein was detected in the cytosol and was associated with ribbon-like structures that resembled membranous organelles. In marked contrast to the U$_L$31 and U$_L$34 gene products, the U$_S$3 protein was clearly associated with viral particles localized at the plasma membrane and extracellular viral particles, as shown in Fig. 5C. This observation is consistent with U$_S$3-specific immunoreactivity detected at the plasma membrane of wild-type-infected cells analyzed by IFA (Fig. 4E). As a negative control, thin sections infected with a U$_S$3-null HSV strain were stained with the U$_S$3 antisera, and they exhibited negligible levels of background immunostaining (Fig. 7B).

The U$_L$31 and U$_L$34 proteins are associated with nuclear membrane invaginations in cells infected with a U$_S$3-null virus. Previous studies utilizing IFA demonstrated that the U$_L$31 and U$_L$34 proteins colocalize in punctate regions associated with the nuclear rim in cells infected with HSV U$_S$3-null mutant viruses. To characterize these structures at the ultrastructural level, Vero cells were infected with the R7037 U$_S$3 mutant virus and subjected to immunogold TEM with antiserum directed against either the U$_L$31 or the U$_L$34 protein as described above. Representative results are shown in Fig. 6 and 7. The morphology of the nuclear membrane in cells infected with the U$_S$3-null HSV strain differed markedly from that of cells infected with HSV-1(F). Specifically, individual thin sections of an entire cell typically contained approximately 5 to 10 clusters of one to several enveloped viral particles along the nuclear rim labeled with U$_L$31 (examples are shown in Fig. 6) and U$_L$34 (an example is shown in Fig. 7A) protein-specific antibodies. The clustered viral particles were completely or partially surrounded by membranous structures. The lumen of
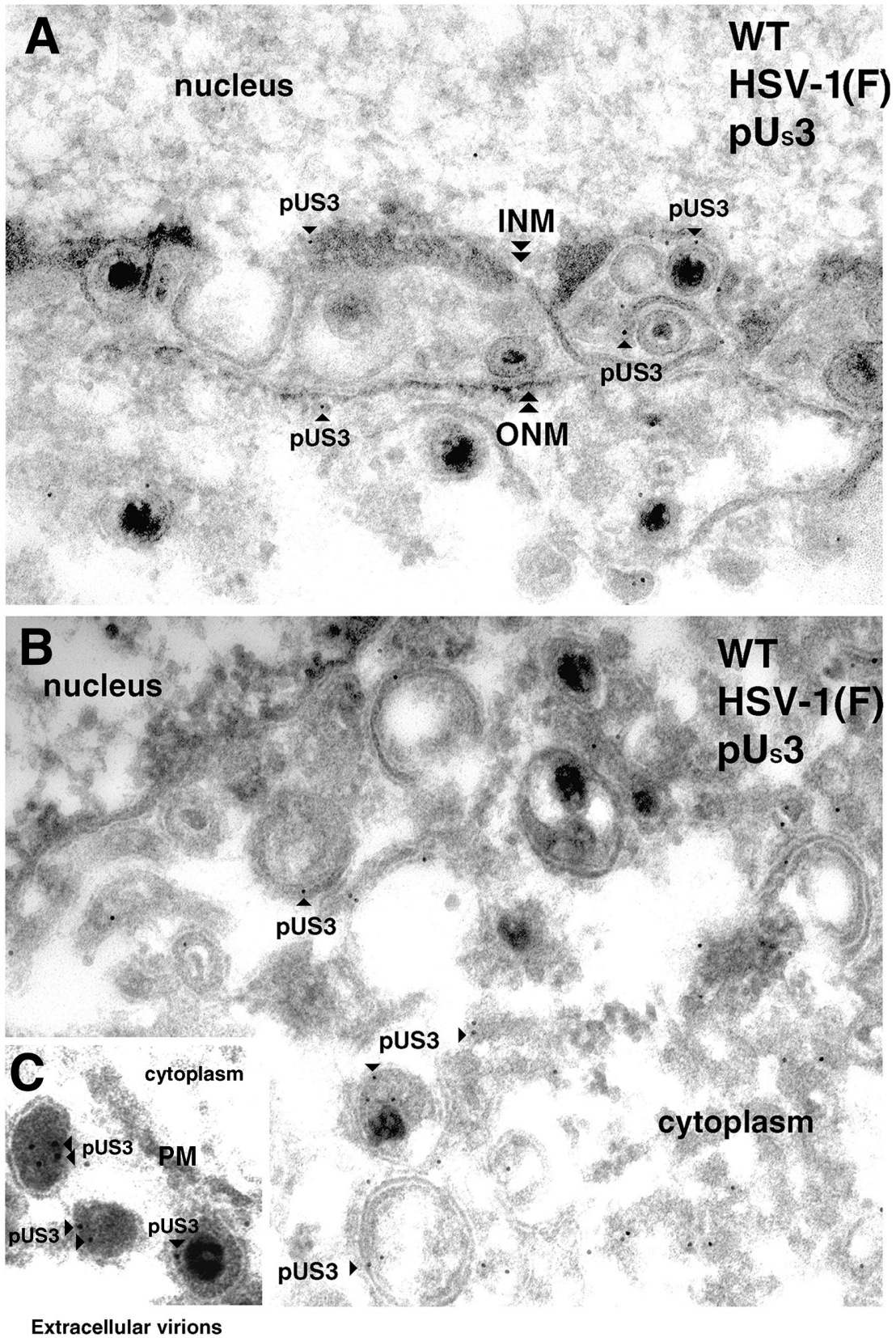
FIG. 5. Digitally scanned electron micrograph of wild-type (WT) virus-infected Vero cells harvested and fixed late in infection. Thin sections were probed with U_S3 protein-specific rabbit polyclonal antisera. Bound antibody is indicated with arrowheads labeled pU_S3. The nucleus is indicated, and the locations of the INM and ONM are indicated by double arrowheads in panel A. In addition to the subcellular structures labeled in panel A, the location of the cytoplasm is indicated in panel B. In panel C, the cytoplasm and plasma membrane (PM) are designated and extracellular virions labeled with pU_S3 are shown. Original magnification of panels A to C, ×45,000.
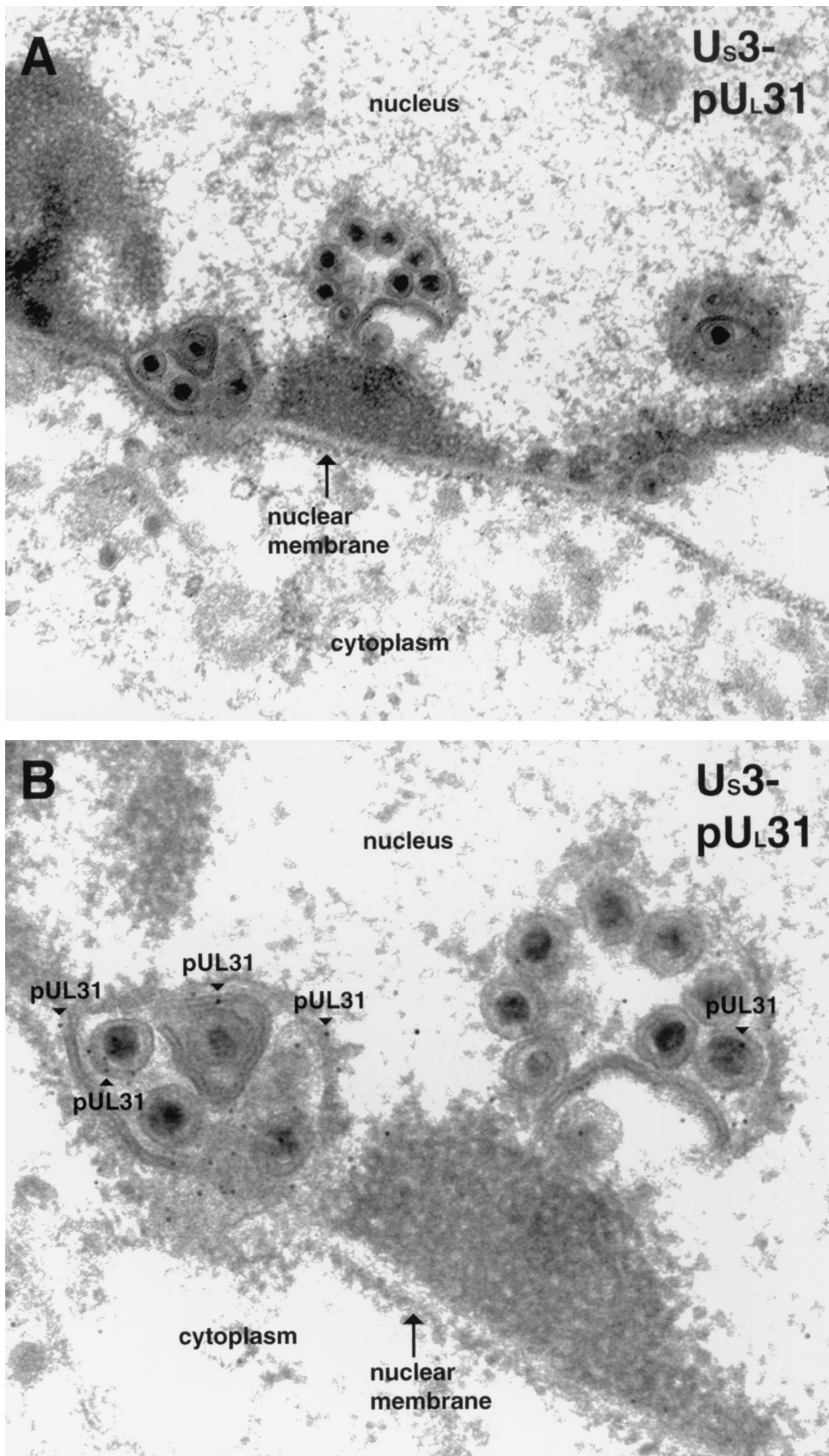
FIG. 6. Digitally scanned image of electron micrographs of U_S3-null mutant virus-infected cells harvested and fixed late in infection. Thin sections were probed with U_L31 protein-specific rabbit polyclonal antisera. Regions labeled with gold beads are marked with arrowheads labeled pU_L31. The nucleus, nuclear membrane, and cytoplasm are labeled in panel A, and the nucleus is designated in panel B. Original magnifications: A, ×30,000; B, ×45,000.
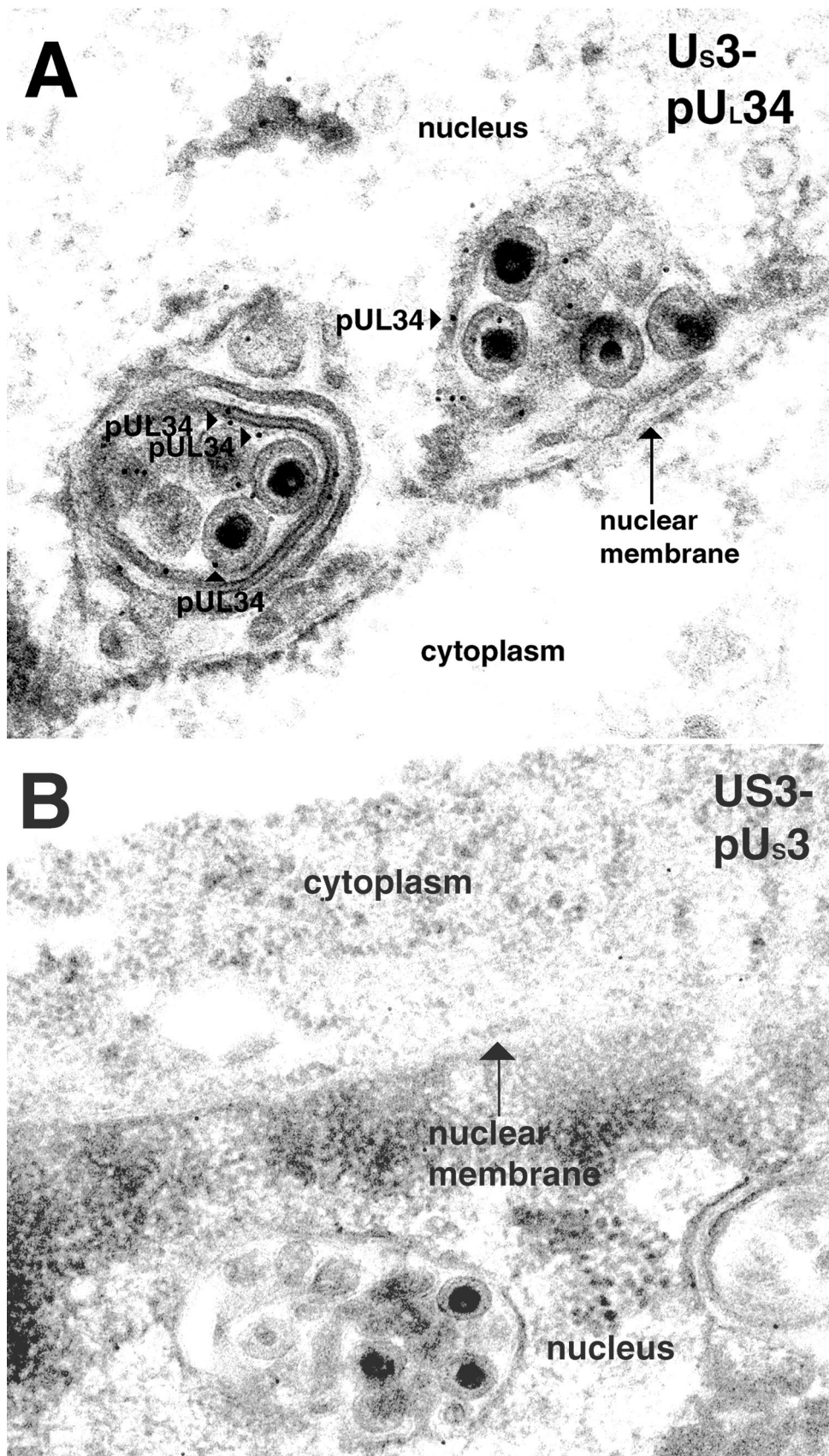
FIG. 7. Scanned digital electron micrograph of thin sections of U_S3-null mutant virus-infected cells incubated with anti-U_L34 chicken IgY. Bound antibody is indicated with pU_L34-labeled arrowheads, and the nucleus and cytoplasm are labeled. In panel B, thin sections of U_S3-null HSV-infected cells were incubated with U_S3 protein-specific rabbit polyclonal antisera. Original magnification of panels A and B, ×45,000.

many of these membrane-bound packets of viral particles was continuous with the nuclear membrane and thus appeared to be an invagination of one or both lamellae of the nuclear envelope.

The U_L31 gene product was located almost exclusively at the nuclear membrane, as in wild-type virus-infected cells. However, the appearance of U_L31 immunostaining in cells infected with the U_S3-null virus differed from that of cells infected with the wild-type virus inasmuch as (i) the distribution largely localized within packets of viral particles at the perinuclear space and (ii) significantly more U_L31 protein-specific immunoreactivity was detected in cells infected with the U_S3-null virus. Specifically, a mean of approximately 230 gold particles was detected per section, as opposed to a mean of approximately 31 gold particles per section of cells infected with HSV-1(F), as shown in Table 1.

In conclusion, cells infected with the U_S3-null mutant virus contain abnormally large numbers of viral particles containing the U_L31 and U_L34 proteins, which are wrapped in one or more layers of nuclear membrane. Very similar structures have been reported in cells infected with a U_S3-null PrV (22). The discrete, nuclear envelope-associated foci of the colocalized U_L31 and U_L34 proteins detected by optical sectioning of U_S3-null HSV-infected cells described previously (32) likely correspond to the virion-containing membranous vesicles characterized by TEM in this study, given that the sizes and numbers of vesicles detected by the two assays are comparable. The observation that many of the membranes surrounded several enveloped virions suggests that particles are delayed in their transit from the nucleus to the cytoplasm and ultimately, to the extracellular space. It is worth noting that the U_S3 kinase does not appear to be required for budding of nucleocapsids through the INM and also is not required for association of the U_L31 and U_L34 proteins with nascent virions in the perinuclear space. One possibility consistent with these observations is that the U_S3 protein is necessary for proper regulation of the deenvelopment of perinuclear virions at the ONM. It is also possible that the Us3-encoded kinase plays a direct or indirect role in facilitating virion transport.

Deletion of the U_S3 ORF impairs growth of HSV on HEp-2 cells. It has been reported that the U_S3-encoded kinase is not essential for growth in tissue culture cells (27). This conclusion was based largely on an experiment in which Vero cells were infected at high and low MOIs with HSV-1(F) and at 48 hpi, the virus yields were determined to be similar for HSV-1(F) and two strains of U_S3-null HSV. Inasmuch as the U_S3-encoded kinase affects the localization of two essential proteins, we have extended that study by determining the single-step growth characteristics of U_S3-null HSV in HEp-2 cells. Replicate confluent monolayers of Vero cells in 12-well dishes were infected at an MOI of 5 for 1 h at 4°C with HSV-1(F) or either of two independently isolated U_S3-null mutant viruses (R7037 and R7039). Each inoculum was then replaced with 37°C V medium (Dulbecco modified Eagle medium supplemented with 5% heat-inactivated calf serum) and incubated at 37°C for 2 h. To remove and inactivate residual virus, infected cells were washed once with 37°C citrate buffer (50 mM sodium citrate, 4 mM KCl [adjusted to pH 3.0 with HCl]) and incubated for 1 min in a second wash of the same buffer. Cells were then washed twice in 37°C V medium and incubated in 2 ml of V
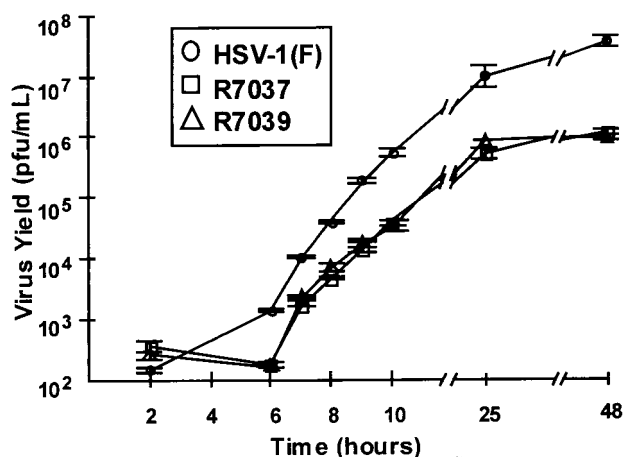

FIG. 8. Single-step growth analysis of HSV-1(F) and two HSV U_S3-null mutant viruses on HEp-2 cells. Replicate cultures of HEp-2 cells were infected with HSV-1(F) or either of two U_S3-null mutant viruses (R7037 and R7039). At the indicated times, cells were harvested and viral yield was determined by titration on Vero cells. Virus yield is expressed as PFU per milliliter of culture medium. Each datum point represents the mean of three independent experiments, and the error bars indicate the sample standard deviation.

medium for the remainder of the infection. At various times, infected cells were frozen at -80°C, subsequently thawed, and then sonicated with a Fisher Sonic Dismembrator at a power level 0 for 30 s to lyse the cells. The infectious virus titer was then determined on Vero cells by plaque assay. The data are shown in Fig. 8.

On HEp-2 cells, HSV-1(F) replication had entered the productive phase by 6 hpi and reached a plateau phase by 25 hpi, with a titer of approximately 10^7 PFU/ml. In contrast, the U_S3-null virus strains did not initiate production of infectious virus until after the 6-h time point and reached plateau titers at 25 hpi of only 6×10^5 and 8×10^5 PFU/ml (R7037 and R7039, respectively). Moreover, the 48-hpi yield of HSV-1(F) was approximately 3.5×10^7 PFU/ml, compared with approximately 1×10^6 PFU/ml for both U_S3-null strains. Each of the U_S3-null viruses used has deletions that affect either the U_S2 or the U_S4 (glycoprotein G) gene. While we cannot exclude the possibility that mutations in U_S2 and U_S4 independently give rise to indistinguishable defects in single-step growth, it seems most likely that the observed growth phenotypes of both viruses are the result of their common failure to express U_S3. These data indicate that, as in Vero cells, the U_S3 ORF is dispensable for growth in HEp-2 cells. However, production of infectious U_S3-null progeny was slightly delayed and peak titers were decreased 10- to 30-fold compared with those of HSV-1(F). In the assay performed, a decreased viral yield could reflect a decrease in virus particle production, egress, or infectivity. However, the observation that deletion of U_S3 delays the onset of infectious virus production favors an impairment of virus particle production or egress over a simple decrease in specific infectivity. Deletion of the U_S3 ORF also results in an altered nuclear rim distribution of U_L31 and U_L34 compared with wild-type virus-infected cells (32). It is possible that the altered distribution of the U_L34 and U_L31 proteins, both of which are involved in viral assembly and egress, results in the growth defect associated with deletion of the U_S3 locus

in HSV. The increase in the total number of U_L31 protein-specific gold beads detected in U_L34-null mutant- and U_S3-null mutant-infected cells compared with wild-type virus-infected cells shown in Table 1 may be (i) reflective of this proposed delay in the egress of virions or (ii) due to direct or indirect effects of the U_S3 protein on the U_L31 or U_L34 protein.

The data reported herein are consistent with reports concerning the U_S3 homologues of other alphaherpesviruses. It has been proposed that the U_S3-encoded kinase of PrV is involved in deenvelopment of perinuclear virions at the ONM (45), and U_S3 deletion mutants of PrV exhibit an approximately 10-fold reduction in viral yield in a cell type-dependent manner (20). Similar results have also been reported for U_S3 deletion mutants of bovine herpesvirus type 1 (42).

REFERENCES

1. **Baines, J. D., and B. Roizman.** 1992. The U_L11 gene of herpes simplex virus 1 encodes a function that facilitates nucleocapsid envelopment and egress from cells. J. Virol. **66:**5168–5174.
2. **Blaho, J., C. Mitchell, and B. Roizman.** 1994. An amino acid sequence shared by the herpes simplex virus 1 alpha regulatory proteins 0, 4, 22, and 27 predicts the nucleotidylylation of the U_L21, U_L31, U_L47, and U_L49 gene products. J. Biol. Chem. **269:**17401–17410.
3. **Browne, H., S. Bell, T. Minson, and D. W. Wilson.** 1996. An endoplasmic reticulum-retained herpes simplex virus glycoprotein H is absent from secreted virions: evidence for reenvelopment during egress. J. Virol. **70:**4311–4316.
4. **Chang, Y. E., and B. Roizman.** 1993. The product of the U_L31 gene of herpes simplex virus 1 is a nuclear phosphoprotein which partitions with the nuclear matrix. J. Virol. **67:**6348–6356.
5. **Chang, Y. E., C. Van Sant, P. W. Krug, A. E. Sears, and B. Roizman.** 1997. The null mutant of the U_L31 gene of herpes simplex virus 1: construction and phenotype in infected cells. J. Virol. **71:**8307–8315.
6. **Darlington, R. W., and L. H. Moss III.** 1968. Herpesvirus envelopment. J. Virol. **2:**48–55.
7. **Ejercito, P. M., E. D. Kieff, and B. Roizman.** 1968. Characterization of herpes simplex virus strains differing in their effects on social behaviour of infected cells. J. Gen. Virol. **2:**357–364.
8. **Enquist, L. W., P. J. Husak, B. W. Banfield, and G. A. Smith.** 1998. Infection and spread of alphaherpesviruses in the nervous system. Adv. Virus Res. **51:**237–347.
9. **Frame, M. C., F. C. Purves, D. J. McGeoch, H. S. Marsden, and D. P. Leader.** 1987. Identification of the herpes simplex virus protein kinase as the product of the viral gene US3. J. Gen. Virol. **68**(Pt. 10)**:**2699–2704.
10. **Fuchs, W., B. G. Klupp, H. Granzow, N. Osterrieder, and T. C. Mettenleiter.** 2002. The interacting UL31 and UL34 gene products of pseudorabies virus are involved in egress from the host-cell nucleus and represent components of primary enveloped but not mature virions. J. Virol. **76:**364–378.
11. **Gershon, A. A., D. L. Sherman, Z. Zhu, C. A. Gabel, R. T. Ambron, and M. D. Gershon.** 1994. Intracellular transport of newly synthesized varicella-zoster virus: final envelopment in the trans-Golgi network. J. Virol. **68:**6372–6390.
12. **Goshima, F., T. Daikoku, H. Yamada, S. Oshima, T. Tsurumi, and Y. Nishiyama.** 1998. Subcellular localization of the US3 protein kinase of herpes simplex virus type 2. Arch. Virol. **143:**613–622.
13. **Granzow, H., F. Weiland, A. Jons, B. G. Klupp, A. Karger, and T. C. Mettenleiter.** 1997. Ultrastructural analysis of the replication cycle of pseudorabies virus in cell culture: a reassessment. J. Virol. **71:**2072–2082.
14. **Granzow, H., B. G. Klupp, W. Fuchs, J. Veits, N. Osterrieder, and T. C. Mettenleiter.** 2001. Egress of alphaherpesviruses: comparative ultrastructural study. J. Virol. **75:**3675–3684.
15. **Hutchinson, L., and D. C. Johnson.** 1995. Herpes simplex virus glycoprotein K promotes egress of virus particles. J. Virol. **69:**5401–5413.
16. **Jayachandra, S., A. Baghian, and K. G. Kousoulas.** 1997. Herpes simplex virus type 1 glycoprotein K is not essential for infectious virus production in actively replicating cells but is required for efficient envelopment and translocation of infectious virions from the cytoplasm to the extracellular space. J. Virol. **71:**5012–5024.
17. **Jerome, K. R., R. Fox, Z. Chen, A. E. Sears, H.-Y. Lee, and L. Corey.** 1999. Herpes simplex virus inhibits apoptosis through the action of two genes, Us5 and Us3. J. Virol. **73:**8950–8957.
18. **Johnson, D. C., and P. G. Spear.** 1982. Monensin inhibits the processing of herpes simplex virus glycoproteins, their transport to the cell surface, and the egress of virions from infected cells. J. Virol. **43:**1102–1112.
19. **Johnson, D. C., M. C. Frame, M. W. Ligas, A. M. Cross, and N. D. Stow.** 1988. Herpes simplex virus immunoglobulin G Fc receptor activity depends on a complex of two viral glycoproteins, gE and gI. J. Virol. **62:**1347–1354.
20. **Kimman, T. G., N. De Wind, T. De Bruin, Y. de Visser, and J. Voermans.** 1994. Inactivation of glycoprotein gE and thymidine kinase or the US3-encoded protein kinase synergistically decrease in vivo replication of pseudorabies virus and the induction of protective immunity. Virology **205:**511–518.
21. **Klupp, B. G., H. Granzow, and T. C. Mettenleiter.** 2000. Primary envelopment of pseudorabies virus at the nuclear membrane requires the UL34 gene product. J. Virol. **74:**10063–10073.
22. **Klupp, B. G., H. Granzow, and T. C. Mettenleiter.** 2001. Effect of the pseudorabies virus US3 protein on nuclear membrane localization of the UL34 protein and virus egress from the nucleus. J. Gen. Virol. **82**(Pt. 10)**:**2363–2371.
23. **Leopardi, R., C. Van Sant, and B. Roizman.** 1997. The herpes simplex virus 1 protein kinase US3 is required for protection from apoptosis induced by the virus. Proc. Natl. Acad. Sci. USA **94:**7891–7896.
24. **Loomis, J. S., J. B. Bowzard, R. J. Courtney, and J. W. Wills.** 2001. Intracellular trafficking of the UL11 tegument protein of herpes simplex virus type 1. J. Virol. **75:**12209–12219.
25. **Mettenleiter, T. C.** 2002. Herpesvirus assembly and egress. J. Virol. **76:**1537–1547.
26. **Munger, J., A. V. Chee, and B. Roizman.** 2001. The U_S3 protein kinase blocks apoptosis induced by the *d*120 mutant of herpes simplex virus 1 at a premitochondrial stage. J. Virol. **75:**5491–5497.
27. **Purves, F. C., R. M. Longnecker, D. P. Leader, and B. Roizman.** 1987. Herpes simplex virus 1 protein kinase is encoded by open reading frame US3 which is not essential for virus growth in cell culture. J. Virol. **61:**2896–2901.
28. **Purves, F. C., D. Spector, and B. Roizman.** 1991. The herpes simplex virus 1 protein kinase encoded by the U_S3 gene mediates posttranslational modification of the phosphoprotein encoded by the U_L34 gene. J. Virol. **65:**5757–5764.
29. **Purves, F. C., D. Spector, and B. Roizman.** 1992. UL34, the target of the herpes simplex virus U_S3 protein kinase, is a membrane protein which in its unphosphorylated state associates with novel phosphoproteins. J. Virol. **66:**4295–4303.
30. **Radsak, K., M. Eickmann, T. Mockenhaupt, E. Bogner, H. Kern, A. Eis-Hubinger, and M. Reschke.** 1996. Retrieval of human cytomegalovirus glycoprotein B from the infected cell surface for virus envelopment. Arch. Virol. **141:**557–572.
31. **Reynolds, A. E., Y. Fan, and J. D. Baines.** 2000. Characterization of the U_L33 gene product of herpes simplex virus 1. Virology **266:**310–318.
32. **Reynolds, A. E., B. J. Ryckman, J. D. Baines, Y. Zhou, L. Liang, and R. J. Roller.** 2001. U_L31 and U_L34 proteins of herpes simplex virus type 1 form a complex that accumulates at the nuclear rim and is required for envelopment of nucleocapsids. J. Virol. **75:**8803–8817.
33. **Roizman, B., and A. E. Sears.** 1996. Herpes simplex viruses and their replication, p. 2221–2278. *In* B. N. Fields, D. M. Knipe, and P. M. Howley (ed.), Fields virology, 3rd ed. Lippincott-Raven, Philadelphia, Pa.
34. **Roller, R. J., Y. Zhou, R. Schnetzer, J. Ferguson, and D. DeSalvo.** 2000. Herpes simplex virus type 1 U_L34 gene product is required for viral envelopment. J. Virol. **74:**117–129.
35. **Schwartz, J., and B. Roizman.** 1969. Concerning the egress of herpes simplex virus from infected cells: electron and light microscope observations. Virology **38:**42–49.
36. **Shiba, C., T. Daikoku, F. Goshima, H. Takakuwa, Y. Yamauchi, O. Koiwai, and Y. Nishiyama.** 2000. The UL34 gene product of herpes simplex virus type 2 is a tail-anchored type II membrane protein that is significant for virus envelopment. J. Gen. Virol. **81**(Pt. 10)**:**2397–2405.
37. **Skepper, J. N., A. Whiteley, H. Browne, and A. Minson.** 2001. Herpes simplex virus nucleocapsids mature to progeny virions by an envelopment → deenvelopment → reenvelopment pathway. J. Virol. **75:**5697–5702.
38. **Smith, S., and G. Blobel.** 1993. The first membrane spanning region of the lamin B receptor is sufficient for sorting to the inner nuclear membrane. J. Cell Biol. **120:**631–637.
39. **Soullam, B., and H. J. Worman.** 1993. The amino-terminal domain of the lamin B receptor is a nuclear envelope targeting signal. J. Cell Biol. **120:**1093–1100.

40. **Soullam, B., and H. J. Worman.** 1995. Signals and structural features involved in integral membrane protein targeting to the inner nuclear membrane. J. Cell Biol. **130:**15–27.

41. **Stackpole, C. W., and M. Mizell.** 1968. Electron microscopic observations on herpes-type virus-related structures in the frog renal adenocarcinoma. Virology **36:**63–72.

42. **Takashima, Y., H. Tamura, X. Xuan, and H. Otsuka.** 1999. Identification of the US3 gene product of BHV-1 as a protein kinase and characterization of BHV-1 mutants of the US3 gene. Virus Res. **59:**23–34.

43. **Taus, N. S., B. Salmon, and J. D. Baines.** 1998. The herpes simplex virus 1 U$_L$17 gene is required for localization of capsids and major and minor capsid proteins to intranuclear sites where viral DNA is cleaved and packaged. Virology **252:**115–125.

44. **Torrisi, M. R., C. Di Lazzaro, A. Pavan, L. Pereira, and G. Campadelli-Fiume.** 1992. Herpes simplex virus envelopment and maturation studied by fracture label. J. Virol. **66:**554–561.

45. **Wagenaar, F., J. M. Pol, B. Peeters, A. L. Gielkens, N. de Wind, and T. G. Kimman.** 1995. The US3-encoded protein kinase from pseudorabies virus affects egress of virions from the nucleus. J. Gen. Virol. **76**(Pt. 7)**:**1851–1859.

46. **Whealy, M. E., J. P. Card, R. P. Meade, A. K. Robbins, and L. W. Enquist.** 1991. Effect of brefeldin A on alphaherpesvirus membrane protein glycosylation and virus egress. J. Virol. **65:**1066–1081.

47. **Whiteley, A., B. Bruun, T. Minson, and H. Browne.** 1999. Effects of targeting herpes simplex virus type 1 gD to the endoplasmic reticulum and trans-Golgi network. J. Virol. **73:**9515–9520.

48. **Yamauchi, Y., C. Shiba, F. Goshima, A. Nawa, T. Murata, and Y. Nishiyama.** 2001. Herpes simplex virus type 2 UL34 protein requires UL31 protein for its relocation to the internal nuclear membrane in transfected cells. J. Gen. Virol. **82**(Pt.6)**:**1423–1428.

49. **Ye, G. J., and B. Roizman.** 2000. The essential protein encoded by the UL31 gene of herpes simplex virus 1 depends for its stability on the presence of UL34 protein. Proc. Natl. Acad. Sci. USA **97:**11002–11007.

50. **Zhu, Z., M. D. Gershon, Y. Hao, R. T. Ambron, C. A. Gabel, and A. A. Gershon.** 1995. Envelopment of varicella-zoster virus: targeting of viral glycoproteins to the trans-Golgi network. J. Virol. **69:**7951–7959.

51. **Zhu, H. Y., H. Yamada, Y. M. Jiang, M. Yamada, and Y. Nishiyama.** 1999. Intracellular localization of the UL31 protein of herpes simplex virus type 2. Arch. Virol. **144:**1923–1935.